scientific reports

Check for updates

OPEN

Two optimized novel potential formulas and numerical algorithms for $m \times n$ cobweb and fan resistor networks

Wenjie Zhao[1], Yanpeng Zheng[1]✉, Xiaoyu Jiang[2] & Zhaolin Jiang[3]✉

The research of resistive network will become the basis of many fields. At present, many exact potential formulas of some complex resistor networks have been obtained. Computer numerical simulation is the trend of computing, but written calculation will limit the time and scale. In this paper, the potential formulas of a $m \times n$ scale cobweb resistor network and fan resistor network are optimized. Chebyshev polynomial of the second class and the absolute value function are used to express the novel potential formulas of the resistor network, and described in detail the derivation process of the explicit formula. Considering the influence of parameters on the potential formulas, several idiosyncratic potential formulas are proposed, and the corresponding three-dimensional dynamic images are drawn. Two numerical algorithms of the computing potential are presented by using the mathematical model and *DST-VI*. Finally, the efficiency of calculating potential by different methods are compared. The advantages of new potential formulas and numerical algorithms by the calculation efficiency of the three methods are shown. The optimized potential formulas and the presented numerical algorithms provide a powerful tool for the field of science and engineering.

Tan[1] creatively established the mathematical model of cobweb and fan resistor networks, according to this model, gave the incomparable analytical potential formula in theory. This is a breakthrough work, and its theoretical significance and application prospects are huge. As is well-known, classical physics is based on the analysis of physics mathematical models of physical processes. Computers have given physicists and engineers a new way to analyze and apply physical formulas and mathematical models that has revolutionized science and engineering outside the university. Everything changes if the computer is used to analyze and apply physical formulas and mathematical models. In addition, experts in engineering and scientific computing know that to improve the computational efficiency of the potential to help computational physicists and engineers solve major scientific and technical problems, it is a good idea to optimize the perfect analytical potential formula given in theory to improve the computational efficiency. In order to improve the calculation performance and scale of the formula. In this paper, based on the original potential formula, we re-represent it with the Chebyshev polynomial of the second class and the absolute value function, which improves the computational efficiency, and design the numerical algorithms can be used to the calculating potential for large-scale resistor networks.

In the process of scientific development, many complex problems have arisen, which often require simple models to solve. According to the research results of resistor network model[2–11] and neural network model[12–18], ideas can be obtained on many complex problems. In the past many years, through the research results of Green's function, Laplace equation, Poisson equation, finite and infinite dimensional resistor network and Laplace matrix (*LM*) method and so on[8–11,19–32], the foundation of resistor network research has been laid. Shi et al.[12,13] studied a new discrete time recurrent neural network and its application to manipulators. Sun et al.[14,15] studied the theory and application of noise tolerance zeroing neural network. And Jin et al.[16–18] proposed a modified Zhang neural network (*MZNN*) model for the solution of time-varying quadratic programing (*TVQP*).

In the past few years, Tan et al.[33–53] proposed a simpler recursive transformation (*RT*) method than *LM* method in the research of resistance network. It simplified the Laplacian matrix in two directions to the Laplacian matrix in one direction. In 2014, Tan et al.[37] solved the potential formula of spherical resistance network for the first time. Since 2015, Tan et al.[34–44] has studied the resistance network model by *RT* method. After 2020,

[1]School of Automation and Electrical Engineering, Linyi University, Linyi 276000, China. [2]School of Information Science and Engineering, Linyi University, Linyi 276000, China. [3]School of Mathematics and Statistics, Linyi University, Linyi 276000, China. ✉email: zhengyanpeng0702@sina.com; jzh1208@sina.com

Tan et al.[45–53] made more in-depth research on resistance network. Since *RT* method requires using a tridiagonal matrix to construct a mathematical model, and the analytical potential formula must be expressed by using the exact eigenvalues of this tridiagonal matrix. So the exact eigenvalues of the tridiagonal matrix need to be found. Tridiagonal matrices are used in many areas of science and engineering, and there are many good conclusions about it[54–61].

In 2017, Tan[1] used *RT*-*V* method for the first time to study cobweb network and fan network. In Figs. 1 and 2, the resistance on the warp and weft lines is r_0 and r, where m and n are the scale of the resistor network, it contains m rows and n columns. Point $O_{(0,0)} = 0$ is defined as the origin of the resistor network. The potential formula $U_{m\times n}(x, y)$ of any node $d(x, y)$ in the $m \times n$ cobweb network is shown as

$$\frac{U_{m\times n}(x,y)}{J} = \frac{4r}{2m+1}\sum_{i=1}^{m}\frac{g^{(i)}_{x_1,x}S_{y_1,i} - g^{(i)}_{x_2,x}S_{y_2,i}}{\lambda_i^n + \bar{\lambda}_i^n - 2}S_{y,i}, \tag{1}$$

$$g^{(i)}_{x_s,x} = F_{n-|x_s-x|} + F_{|x_s-x|}. \tag{2}$$

The potential formula $U_{m\times n}(x, y)$ of any node $d(x, y)$ in the $m \times n$ fan network is shown as

$$\frac{U_{m\times n}(x,y)}{J} = \frac{4r}{2m+1}\sum_{i=1}^{m}\frac{\beta^{(i)}_{x_1,x}S_{y_1,i} - \beta^{(i)}_{x_2,x}S_{y_2,i}}{(t_i-2)F^{(i)}_{n+1}}S_{y,i}, \tag{3}$$

$$\beta^{(i)}_{x_s,x} = \begin{cases} \Delta F^{(i)}_{x_s}\Delta F^{(i)}_{n-x} & if\ x \geq x_s, \\ \Delta F^{(i)}_{x}\Delta F^{(i)}_{n-x_s} & if\ x \leq x_s, \end{cases} \tag{4}$$

where $\theta_i = \frac{(2i-1)\pi}{(2m+1)}$, $S_{y_k,i} = \sin(y_k\theta_i)$

$$F^{(i)}_k = \frac{\lambda_i^k - \bar{\lambda}_i^k}{\lambda_i - \bar{\lambda}_i}, \tag{5}$$

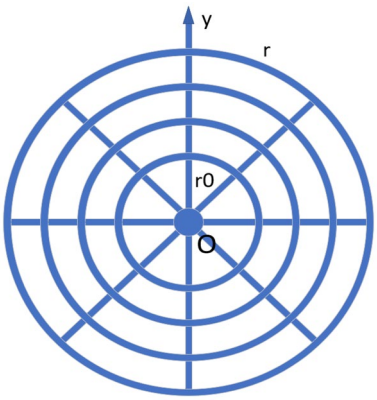

Figure 1. A 8 × 4 cowbeb resistor network containing 8 × 4 nodes and a zero potential point *O*.

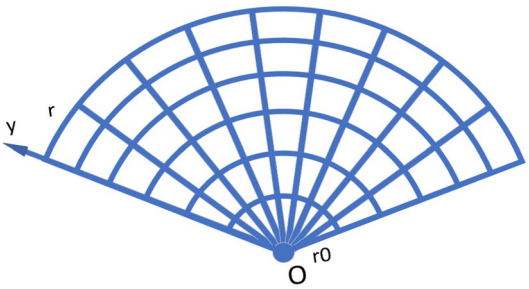

Figure 2. A 10 × 6 fan resistor network containing 10 × 6 nodes and a zero potential point *O*.

$$\begin{aligned}\lambda_i &= 1+h-h\cos\theta_i+\sqrt{(1+h-h\cos\theta_i)^2-1},\\ \bar{\lambda}_i &= 1+h-h\cos\theta_i-\sqrt{(1+h-h\cos\theta_i)^2-1},\end{aligned} \tag{6}$$

$$t_i = 2+2h-2h\cos\theta_i, \tag{7}$$

the parameter $h=\frac{r}{r_0}$ is defined.

Novel formulas of potential represented by Chebyshev polynomials

This section presents the re-expressed potential formulas (1) and (3)[1] of the resistor network. The potential formula expressed by the Chebyshev polynomial of the second class[62] can reduce the running time of computer simulation.

Assume that the current J is input from $d_1(x_1,y_1)$ and output from $d_2(x_2,y_2)$. The potential formula of any node $d(x,y)$ in the $m\times n$ cobweb resistor network is

$$\frac{\mathbf{U}_{m\times n}(x,y)}{J} = \frac{4r}{2m+1}\sum_{\iota=1}^{m}\frac{\mu^{(\iota)}_{x_1,x}S_{y_1,\iota}-\mu^{(\iota)}_{x_2,x}S_{y_2,\iota}}{U^{(\iota)}_n-U^{(\iota)}_{n-2}-2}S_{y,\iota}, \tag{8}$$

where

$$\mu^{(\iota)}_{x_s,x} = U^{(\iota)}_{n-|x_s-x|-1}+U^{(\iota)}_{|x_s-x|-1},\ \ s=1,\ 2. \tag{9}$$

The potential formula of any node $d(x,y)$ in the $m\times n$ fan resistor network is

$$\frac{\mathcal{U}_{m\times n}(x,y)}{J} = \frac{4r}{2m+1}\sum_{\iota=1}^{m}\frac{\varepsilon^{(\iota)}_{x_1,x}S_{y_1,\iota}-\varepsilon^{(\iota)}_{x_2,x}S_{y_2,\iota}}{(\omega_\iota-2)U^{(\iota)}_n}S_{y,\iota}, \tag{10}$$

where

$$\varepsilon^{(\iota)}_{x_s,x} = (U^{(\iota)}_{-0.5})^2(U^{(\iota)}_{n-|x_s-x|+1}-U^{(\iota)}_{n-|x_s-x|-1}+U^{(\iota)}_{n-x_s-x}-U^{(\iota)}_{n-x_s-x-2}),\ \ s=1,\ 2, \tag{11}$$

$$S_{y_k,\iota} = \sin(\frac{y_k(2\iota-1)\pi}{2m+1}),\ \ k=1,\ 2, \tag{12}$$

$$\omega_\iota = 2+\frac{2r}{r_0}-\frac{2r}{r_0}\cos\frac{(2\iota-1)\pi}{2m+1}, \tag{13}$$

$$U^{(\iota)}_\nu = U^{(\iota)}_\nu(\cosh\phi_\iota) = \frac{\sinh(\nu+1)\phi_\iota}{\sinh(\phi_\iota)}, \cosh\phi_\iota = \frac{\omega_\iota}{2},\ \ \frac{\omega_\iota}{2}>1,\ \ \phi_\iota>0, \tag{14}$$

$$\begin{aligned}&\nu = n-|x_s-x|-1,\ |x_s-x|-1,\ n-2,\ n-|x_s-x|+1,\ n-x_s-x,\\ &\quad n-x_s-x-2,\ n,\ -0.5,\ \ s=1,\ 2,\ \ \iota=1,\ 2,\ldots,\ m.\end{aligned}$$

We set the node voltage at point $O_{(0,0)}$ to 0, and the formula for calculating the potential of any node is described as

$$\mathbf{U}_{m\times n}(x,y) = \mathbf{V}^{(y)}_x,\ \mathcal{U}_{m\times n}(x,y) = \mathcal{V}^{(y)}_x,\ \ V^{(0)}_0 = 0, \tag{15}$$

where $\mathbf{V}^{(y)}_x$ and $\mathcal{V}^{(y)}_x$ are denoted by the node voltage of any node.

Horadam sequence and discrete sine transform

In this section, we introduce the explicit formula of Horadam sequence which is expressed by the Chebyshev polynomial of the second class and the sixth kind of discrete sine transform.

A second-order recurrence sequence W_ν is called a Horadam sequence if

$$W_\nu = dW_{\nu-1}-qW_{\nu-2},\ \ W_0=a,\ \ W_1=b, \tag{16}$$

where $\nu\in\mathbf{N},\ \ \nu\geq 2,\ \ a,\ b,\ d,\ q\in\mathbb{C}$, $\mathbf{N}$ is set of all nonnegative integers and $\mathbb{C}$ is the set of all complex numbers.

The explicit formula of Horadam sequence expressed by the Chebyshev polynomial of the second class is[63]

$$W_\nu = (\sqrt{q})^\nu\left(\frac{b}{\sqrt{q}}U_{\nu-1}\left(\frac{d}{2\sqrt{q}}\right)-aU_{\nu-2}\left(\frac{d}{2\sqrt{q}}\right)\right), \tag{17}$$

where U_ν is the Chebyshev polynomial of the second class[62], i.e.

$$U_v = U_v(\cos\phi) = \frac{\sin(v+1)\phi}{\sin\phi}, \quad \cos\phi = \frac{d}{2\sqrt{q}}, \quad \phi \in \mathbb{C}. \tag{18}$$

If $\frac{d}{2\sqrt{q}} > 1$, the Chebyshev polynomial of the second class is re-described by hyperbolic functions, then Eq. (18) is transformed into

$$U_v = U_v(\cosh\phi) = \frac{\sinh(v+1)\phi}{\sinh\phi}, \quad \cosh\phi = \frac{d}{2\sqrt{q}}, \quad \phi \in \mathbb{R}, \tag{19}$$

where $\mathbb{R}$ is the set of all real numbers.

First, we will present the derivation of Eq. (5) represented by the Chebyshev polynomial of the second class.

Remark 1 It can be obtained from Eq. (6) that $\lambda_\iota + \bar{\lambda}_\iota = \omega_\iota$ and $\lambda_\iota \cdot \bar{\lambda}_\iota = 1$. Adding these conditions to Eq. (16), we get the following special Horadam sequence

$$F_v^{(\iota)} = \omega_\iota F_{v-1}^{(\iota)} - F_{v-2}^{(\iota)}, \quad F_0^{(\iota)} = 0, \quad F_1^{(\iota)} = 1, \tag{20}$$

where $d = \omega_\iota > 2$, $q = 1$, $F_v^{(\iota)}$ and ω_ι are expressed in Eqs. (5) and (13), respectively. By replacing the expression of Eq. (5), with the results of Eq. (19), we have

$$F_v^{(\iota)} = \frac{\lambda_\iota^v - \bar{\lambda}_\iota^v}{\lambda_\iota - \bar{\lambda}_\iota} = U_{v-1}^{(\iota)}(\frac{\omega_\iota}{2}). \tag{21}$$

Secondly, we will give the derivation of $\lambda_\iota^n + \bar{\lambda}_\iota^n$ expressed by the Chebyshev polynomial of the second class.

Remark 2 Let

$$B_n^{(\iota)} = \lambda_\iota^n + \bar{\lambda}_\iota^n, \tag{22}$$

where $B_0^{(\iota)} = 2$, $B_1^{(\iota)} = \omega_\iota$.

Then the recursive relation of $B_n^{(\iota)}$ is expressed as

$$B_n^{(\iota)} = \omega_\iota B_{n-1}^{(\iota)} - B_{n-2}^{(\iota)}, \quad B_0^{(\iota)} = 2, \; B_1^{(\iota)} = \omega_\iota, \tag{23}$$

where $d = \omega_\iota$, $q = 1$, ω_ι and $B_n^{(\iota)}$ are expressed in Eqs. (13) and (22), respectively.

By Eqs. (17) and (19), $B_n^{(\iota)}$ is represented as follows

$$B_n^{(\iota)} = \lambda_\iota^n + \bar{\lambda}_\iota^n = \omega_\iota U_{n-1}(\frac{\omega_\iota}{2}) - 2U_{n-2}(\frac{\omega_\iota}{2}) = U_n(\frac{\omega_\iota}{2}) - U_{n-2}(\frac{\omega_\iota}{2}). \tag{24}$$

Next, we will show the derivation of replacing Eq. (4) in terms of piecewise functions with Eq. (11) in terms of absolute value functions.

Remark 3 For Eq. (4), when $x \geq x_s$

Similarly, when $x \leq x_s$

$$\begin{aligned}
\beta_{x_s,x}^{(\iota)} &= (F_{x_s+1}^{(\iota)} - F_{x_s}^{(\iota)})(F_{n-x+1}^{(\iota)} - F_{n-x}^{(\iota)}) \\
&= \left(\frac{\lambda_\iota^{n-x+x_s+2} + \bar{\lambda}_\iota^{n-x+x_s+2} - \lambda_\iota^{n-x+x_s+1} - \bar{\lambda}_\iota^{n-x+x_s+1}}{(\lambda_\iota - \bar{\lambda}_\iota)^2} - \frac{\lambda_\iota^{n-x+x_s+1} + \bar{\lambda}_\iota^{n-x+x_s+1} - \lambda_\iota^{n-x+x_s} - \bar{\lambda}_\iota^{n-x+x_s}}{(\lambda_\iota - \bar{\lambda}_\iota)^2} \right) \\
&\quad + \left(\frac{\lambda_\iota^{n-x-x_s+1} + \bar{\lambda}_\iota^{n-x-x_s+1} - \lambda_\iota^{n-x-x_s} - \bar{\lambda}_\iota^{n-x-x_s}}{(\lambda_\iota - \bar{\lambda}_\iota)^2} - \frac{\lambda_\iota^{n-x-x_s} + \bar{\lambda}_\iota^{n-x-x_s} - \lambda_\iota^{n-x-x_s-1} - \bar{\lambda}_\iota^{n-x-x_s-1}}{(\lambda_\iota - \bar{\lambda}_\iota)^2} \right) \\
&= \left(\frac{(\lambda_\iota - 1)\lambda_\iota^{n-x+x_s+1} + (\bar{\lambda}_\iota - 1)\bar{\lambda}_\iota^{n-x+x_s+1} - (1 - \bar{\lambda}_\iota)\lambda_\iota^{n-x+x_s+1} - (1 - \lambda_\iota)\bar{\lambda}_\iota^{n-x+x_s+1}}{(\lambda_\iota - \bar{\lambda}_\iota)^2} \right) \\
&\quad + \left(\frac{(\lambda_\iota - 1)\lambda_\iota^{n-x-x_s} + (\bar{\lambda}_\iota - 1)\bar{\lambda}_\iota^{n-x-x_s} - (1 - \bar{\lambda}_\iota)\lambda_\iota^{n-x-x_s} - (1 - \lambda_\iota)\bar{\lambda}_\iota^{n-x-x_s}}{(\lambda_\iota - \bar{\lambda}_\iota)^2} \right) \\
&= \frac{(\lambda_\iota + \bar{\lambda}_\iota - 2)(\lambda_\iota^{n-x+x_s+1} + \bar{\lambda}_\iota^{n-x+x_s+1} + \lambda_\iota^{n-x-x_s} + \bar{\lambda}_\iota^{n-x-x_s})}{(\lambda_\iota - \bar{\lambda}_\iota)^2} \\
&= \frac{(\lambda_\iota^{0.5} - \bar{\lambda}_\iota^{0.5})^2}{(\lambda_\iota - \bar{\lambda}_\iota)^2} \left(\lambda_\iota^{n-x+x_s+1} + \bar{\lambda}_\iota^{n-x+x_s+1} + \lambda_\iota^{n-x-x_s} + \bar{\lambda}_\iota^{n-x-x_s} \right) \\
&= (F_{0.5}^{(\iota)})^2 (F_{n-(x-x_s)+2}^{(\iota)} - F_{n-(x-x_s)}^{(\iota)} + F_{n-x-x_s+1}^{(\iota)} - F_{n-x-x_s-1}^{(\iota)}).
\end{aligned} \tag{25}$$

$$
\begin{aligned}
\beta^{(\iota)}_{x_s,x} =&(F^{(\iota)}_{x+1} - F^{(\iota)}_{x})(F^{(\iota)}_{n-x_s+1} - F^{(\iota)}_{n-x_s})\\
=&\left(\frac{\lambda_\iota^{n-x_s+x+2} + \bar{\lambda}_\iota^{n-x_s+x+2} - \lambda_\iota^{n-x_s+x+1} - \bar{\lambda}_\iota^{n-x_s+x+1}}{(\lambda_\iota - \bar{\lambda}_\iota)^2} - \frac{\lambda_\iota^{n-x_s+x+1} + \bar{\lambda}_\iota^{n-x_s+x+1} - \lambda_\iota^{n-x_s+x} - \bar{\lambda}_\iota^{n-x_s+x}}{(\lambda_\iota - \bar{\lambda}_\iota)^2}\right)\\
&+\left(\frac{\lambda_\iota^{n-x_s-x+1} + \bar{\lambda}_\iota^{n-x_s-x+1} - \lambda_\iota^{n-x_s-x} - \bar{\lambda}_\iota^{n-x_s-x}}{(\lambda_\iota - \bar{\lambda}_\iota)^2} - \frac{\lambda_\iota^{n-x_s-x} + \bar{\lambda}_\iota^{n-x_s-x} - \lambda_\iota^{n-x_s-x-1} - \bar{\lambda}_\iota^{n-x_s-x-1}}{(\lambda_\iota - \bar{\lambda}_\iota)^2}\right)\\
=&\left(\frac{(\lambda_\iota - 1)\lambda_\iota^{n-x_s+x+1} + (\bar{\lambda}_\iota - 1)\bar{\lambda}_\iota^{n-x_s+x+1} - (1 - \bar{\lambda}_\iota)\lambda_\iota^{n-x_s+x+1} - (1 - \lambda_\iota)\bar{\lambda}_\iota^{n-x_s+x+1}}{(\lambda_\iota - \bar{\lambda}_\iota)^2}\right)\\
&+\left(\frac{(\lambda_\iota - 1)\lambda_\iota^{n-x_s-x} + (\bar{\lambda}_\iota - 1)\bar{\lambda}_\iota^{n-x_s-x} - (1 - \bar{\lambda}_\iota)\lambda_\iota^{n-x_s-x} - (1 - \lambda_\iota)\bar{\lambda}_\iota^{n-x_s-x}}{(\lambda_\iota - \bar{\lambda}_\iota)^2}\right)\\
=&\frac{(\lambda_\iota + \bar{\lambda}_\iota - 2)(\lambda_\iota^{n-x_s+x+1} + \bar{\lambda}_\iota^{n-x_s+x+1} + \lambda_\iota^{n-x_s-x} + \bar{\lambda}_\iota^{n-x_s-x})}{(\lambda_\iota - \bar{\lambda}_\iota)^2}\\
=&\frac{(\lambda_\iota^{0.5} - \bar{\lambda}_\iota^{0.5})^2}{(\lambda_\iota - \bar{\lambda}_\iota)^2}(\lambda_\iota^{n-x_s+x+1} + \bar{\lambda}_\iota^{n-x_s+x+1} + \lambda_\iota^{n-x_s-x} + \bar{\lambda}_\iota^{n-x_s-x})\\
=&(F^{(\iota)}_{0.5})^2(F^{(\iota)}_{n-(x_s-x)+2} - F^{(\iota)}_{n-(x_s-x)} + F^{(\iota)}_{n-x_s-x+1} - F^{(\iota)}_{n-x_s-x-1}).
\end{aligned}
\tag{26}
$$

Combining Eqs. (25) and (26), Eq. (4) is re-expressed by the absolute value functions as

$$
\beta^{(i)}_{x_s,x} = (F^{(\iota)}_{0.5})^2(F^{(\iota)}_{n-|x_s-x|+2} - F^{(\iota)}_{n-|x_s-x|} + F^{(\iota)}_{n-x_s-x+1} - F^{(\iota)}_{n-x_s-x-1}),\ \ s = 1,\ 2, \tag{27}
$$

By Eqs. (21), (27) and (11) in terms of the Chebyshev polynomial of the second class and absolute value function is obtained.

Using Eqs. (19), (21) and (24), the potential formulas (8) and (10) are obtained.

In order to achieve the fast calculation of numerical simulation, we utilize the sixth kind of discrete sine transform to diagonalize the perturbed tridiagonal matrix $\mathbf{A}_m$[1].

$$
\mathbf{A}_m = \begin{pmatrix}
2+2h & -h & 0 & \cdots & 0\\
-h & 2+2h & -h & \ddots & \vdots\\
0 & \ddots & \ddots & \ddots & 0\\
\vdots & \ddots & -h & 2+2h & -h\\
0 & \cdots & 0 & -h & 2+h
\end{pmatrix}_{m\times m}, \tag{28}
$$

where $h = \frac{r}{r_0}$.

The eigenvectors $\omega_1, \ldots, \omega_m$ of matrix $\mathbf{A}_m$ are expressed as

$$
\omega_\iota = 2 + 2h - 2h\cos\frac{(2\iota - 1)\pi}{2m+1}),\ \ \iota = 1,\ 2, \ldots,\ m, \tag{29}
$$

and the corresponding eigenvectors $\alpha^{(j)} = (\alpha^{(j)}_1, \alpha^{(j)}_2, \ldots, \alpha^{(j)}_m)^T$ are expressed as

$$
\alpha^{(j)}_k = \frac{2}{\sqrt{2m+1}}\sin\frac{(2j-1)k\pi}{2m+1},\ \ k = 1,\ 2, \ldots,\ m,\ \ j = 1,\ 2, \ldots,\ m. \tag{30}
$$

As is known to all, if the orthogonal matrix $\mathbb{S}^{VI}_m$ is the sixth kind of discrete sine transform (*DST-VI*)[64–68], where

$$
\mathbb{S}^{VI}_m = \frac{2}{\sqrt{2m+1}}\left(\sin\frac{(2j-1)k\pi}{2m+1}\right)^m_{k,j=1}, \tag{31}
$$

then

$$
(\mathbb{S}^{VI}_m)^{-1} = (\mathbb{S}^{VI}_m)^T = \mathbb{S}^{VII}_m, \tag{32}
$$

where $(\mathbb{S}^{VI}_m)^T$ is the transpose of the matrix $\mathbb{S}^{VI}_m$ and $\mathbb{S}^{VII}_m$ is the seventh kind of discrete sine transform (*DST-VII*).

The process of realizing the orthogonal diagonalization of matrix $\mathbf{A}_m$ by $\mathbb{S}^{VI}_m$ is as follows

$$
(\mathbb{S}^{VI}_m)^{-1}\mathbf{A}_m(\mathbb{S}^{VI}_m) = \mathrm{diag}(\omega_1, \omega_2, \ldots, \omega_\mathrm{m}), \tag{33}
$$

i.e.,

$$
\mathbf{A}_m = (\mathbb{S}^{VI}_m)\mathrm{diag}(\omega_1, \omega_2, \ldots, \omega_\mathrm{m})(\mathbb{S}^{\mathrm{VI}}_\mathrm{m})^{-1}, \tag{34}
$$

where ω_ι is given by Eq. (29).

By Kirchhoff' s law and the node voltage, Tan[1] gave a matrix equation model as follows

$$\mathbf{V}_{v+1} = \mathbf{A}_m \mathbf{V}_v - \mathbf{V}_{v-1} - r\mathbf{I}_v, \tag{35}$$

where $\mathbf{A}_m$ in Eq. (28), $\mathbf{V}_v$ and $\mathbf{I}_v$ are vectors of length $m \times 1$, in which $\delta_{k,v}(v = k) = 1, \delta_{k,v}(v \neq k) = 0$.

$$\mathbf{V}_v = [V_v^{(1)}, V_v^{(2)}, ...V_v^{(m)}]^T \ (0 \leq v \leq n), \tag{36}$$

$$I_v^{(\iota)} = J(\delta_{x_1,v} - \delta_{x_2,v}). \tag{37}$$

Since Eq. (35) cannot be directly calculated. Equation (35) is transformed by $\mathbb{S}_m^{VI}$ method. The process of transformation is as follows.

$$(\mathbb{S}_m^{VI})^{-1}\mathbf{V}_v = (\mathbb{S}_m^{VI})^T\mathbf{V}_v = \mathbf{C}_v, \ \ \mathbf{V}_v = \mathbb{S}_m^{VI}\mathbf{C}_v, \tag{38}$$

where $\mathbf{C}_v$ is also a $m \times 1$ vector

$$\mathbf{C}_v = [c_v^{(1)}, c_v^{(2)}, ..., c_v^{(m)}]^T \ \ (0 \leq v \leq n). \tag{39}$$

Remark 4 Tan[1] proposed the node voltage formula of the cobweb network as follows

$$V_k^{(y)} = J\frac{4r}{2m+1}\sum_{i=1}^{m}\frac{g_{x_1,x}^{(i)}S_{y_1,i} - g_{x_2,x}^{(i)}S_{y_2,i}}{\lambda_i^n + \bar{\lambda}_i^n - 2}\sin(y\theta_i), \tag{40}$$

where $g_{x_1,x}^{(i)}$ is expressed in Eq. (2), λ_i^n and $\bar{\lambda}_i^n$ is in Eq. (6), $\theta_i = \frac{(2i-1)\pi}{(2m+1)}$, $S_{y_k,i} = \sin(y_k\theta_i), \ k = 1, \ 2$.

According to Eqs. (2), (21), (24) and (40), we re-express the node voltage formula by the Chebyshev polynomial of the second class as follows

$$\mathbf{V}_v^{(y)} = J\frac{4r}{2m+1}\sum_{\iota=1}^{m}\frac{\mu_{x_1,x}^{(\iota)}S_{y_1,\iota} - \mu_{x_2,x}^{(\iota)}S_{y_2,\iota}}{U_n^{(\iota)} - U_{n-2}^{(\iota)} - 2}S_{y,\iota}, \tag{41}$$

where $\mu_{x_s,x}^{(\iota)}, \ s = 1, \ 2$ is same as Eq. (9), $U_v^{(\iota)}$ is same as Eq. (14), and $S_{y_s,\iota}$ is same as Eq. (12).

According to Eqs. (38), (39) and (41), we can get the analytic formula of $\mathbf{c}_x^{(\iota)}$ as

$$\mathbf{c}_x^{(\iota)} = \frac{2rJ}{\sqrt{2m+1}}\left(\frac{\mu_{x_1,x}^{(\iota)}S_{y_1,\iota} - \mu_{x_2,x}^{(\iota)}S_{y_2,\iota}}{U_n^{(\iota)} - U_{n-2}^{(\iota)} - 2}\right), \ \ (0 \leq x \leq n), \tag{42}$$

Tan[1] proposed the node voltage formula of the fan network as follows

$$V_k^{(y)} = J\frac{4r}{2m+1}\sum_{i=1}^{m}\frac{\beta_{x_1,x}^{(i)}S_{y_1,i} - \beta_{x_2,x}^{(i)}S_{y_2,i}}{(t_i - 2)F_{n+1}^{(i)}}\sin(y\theta_i), \tag{43}$$

where $\beta_{x_s,x}^{(i)}$ is expressed in Eq. (4), $F_k^{(i)}$ is given in Eq. (5), t_i is given in Eq. (7), $\theta_i = \frac{(2i-1)\pi}{(2m+1)}$, $S_{y_k,i} = \sin(y_k\theta_i), \ k = 1, \ 2$.

According to Eqs. (4), (7), (13), (21) and (43), we re-express the node voltage formula by the Chebyshev polynomial of the second class as follows

$$\mathcal{V}_v^{(y)} = J\frac{4r}{2m+1}\sum_{\iota=1}^{m}\frac{\varepsilon_{x_1,x}^{(\iota)}S_{y_1,\iota} - \varepsilon_{x_2,x}^{(\iota)}S_{y_2,\iota}}{(\omega_\iota - 2)U_n^{(\iota)}}S_{y,\iota}, \tag{44}$$

where $\varepsilon_{x_s,x}^{(\iota)}, \ s = 1, \ 2$ is same as Eq. (11), $S_{y_s,\iota}$ is same as Eq. (12), ω_ι is same as Eq. (13) and $U_v^{(\iota)}$ is same as Eq. (14).

According to Eqs. (38), (39) and (44), we can get the analytic formula of $c_x^{(\iota)}$ as

$$c_x^{(\iota)} = \frac{2rJ}{\sqrt{2m+1}}\left(\frac{\varepsilon_{x_1,x}^{(\iota)}S_{y_1,\iota} - \varepsilon_{x_2,x}^{(\iota)}S_{y_2,\iota}}{(\omega_\iota - 2)U_n^{(\iota)}}\right), \ \ (0 \leq x \leq n), \tag{45}$$

Displaying of some special and interesting potential formulae

According to the obtained resistor network potential formulas (8) and (10) which contain multiple variables, this chapter analyzed the influence of different variables on the resistance network potential formula from two directions, assigned corresponding variables according to the conditions, and drew a three-dimensional dynamic view intuitive display.

Idiosyncratic potential formulas with the change of current input point and output point position. This section discusses the influence of changes in the position of the input and output points of the current in the resistor network on the potentials, as reflected in the three-dimensional dynamic view.

Idiosyncratic potential formula 1. If the current J flows in point $d_1(x_1, y_1)$ and out of $d_2(x_2, y_2) = O_{(0,0)}$, then a novel potential formula of the cobweb resistor network can be rewritten as

$$\frac{\mathbf{U}_{m\times n}(x,y)}{J}=\frac{4r}{2m+1}\sum_{\iota=1}^{m}\frac{\mu_{x_1,x}^{(\iota)}S_{y_1,\iota}}{U_n^{(\iota)}-U_{n-2}^{(\iota)}-2}S_{y,\iota}, \tag{46}$$

and a novel potential formula of the fan resistor network can be rewritten as

$$\frac{\mathcal{U}_{m\times n}(x,y)}{J}=\frac{4r}{2m+1}\sum_{\iota=1}^{m}\frac{\varepsilon_{x_1,x}^{(\iota)}S_{y_1,\iota}-\varepsilon_{x_2,x}^{(\iota)}S_{y_2,\iota}}{(\omega_\iota-2)U_n^{(\iota)}}S_{y,\iota}, \tag{47}$$

where $\mu_{x_s,x}^{(\iota)},\ s=1,\ 2$ is defined in Eq. (9), $\varepsilon_{x_s,x}^{(\iota)},\ s=1,\ 2$, is defined in Eq. (11), $U_v^{(\iota)}$ is defined in Eq. (14), and $S_{y_s,\iota}$ is defined in Eq. (12).

Let $m=n=60,\ J=10,\ x_1=y_1=20,\ x_2=y_2=0$, and $r_0=r=1$ in Eqs. (46) and (47), respectively. Then a special potential formula of the cobweb resistor network is obtained as follows

$$\frac{\mathbf{U}_{60\times 60}(x,y)}{J}=\frac{4}{121}\sum_{\iota=1}^{60}\frac{\mu_{20,x}^{(\iota)}S_{20,\iota}}{U_{60}^{(\iota)}-U_{58}^{(\iota)}-2}S_{y,\iota}, \tag{48}$$

and a special potential formula of the fan resistor network is obtained as follows

$$\frac{\mathcal{U}_{60\times 60}(x,y)}{J}=\frac{4}{121}\sum_{\iota=1}^{60}\frac{\varepsilon_{20,x}^{(\iota)}S_{20,\iota}}{(\omega_\iota-2)U_{60}^{(\iota)}}S_{y,\iota}, \tag{49}$$

where

$$\mu_{20,x}^{(\iota)}=U_{59-|20-x|}^{(\iota)}+U_{|20-x|-1}^{(\iota)}, \tag{50}$$

$$\varepsilon_{20,x}^{(\iota)}=(U_{-0.5}^{(\iota)})^2(U_{61-|20-x|}^{(\iota)}-U_{59-|20-x|}^{(\iota)}+U_{40-x}^{(\iota)}-U_{38-x}^{(\iota)}), \tag{51}$$

$$\omega_\iota=4-2\cos\frac{(2\iota-1)\pi}{121}, \tag{52}$$

$$S_{20,\iota}=\sin(\frac{(40\iota-20)\pi}{121}), \tag{53}$$

$$U_v^{(\iota)}=U_v^{(\iota)}(\cosh\phi_\iota)=\frac{\sinh(v+1)\phi_\iota}{\sinh(\phi_\iota)},\ \cosh\phi_\iota=\frac{\omega_\iota}{2}, \tag{54}$$

$$S_{y,\iota}=\sin\left(\frac{y(2\iota-1)\pi}{121}\right), \tag{55}$$

$$v=61-|20-x|,\ 59-|20-x|,\ |20-x|-1,\ 40-x,\ 38-x,\ 60,\ 58,\ -0.5.\ \iota=1,\ 2,\ldots,\ 60.$$

And the three-dimensional dynamic views for the generative process of the potential graph are shown in Figs. 3 and 4, respectively.

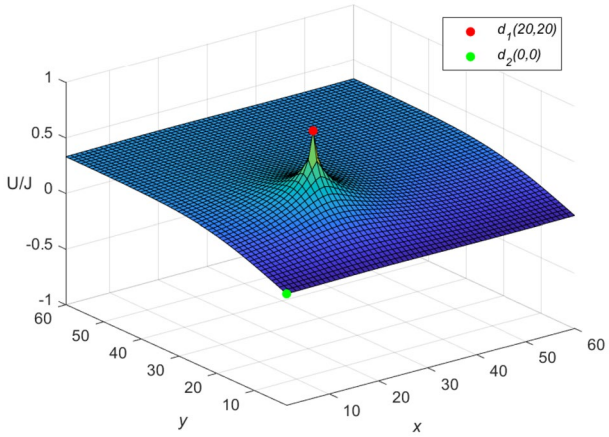

Figure 3. The potential graph for $\mathbf{U}_{60\times 60}(x,y)/J$ with the cobweb resistor network in Eq. (48).

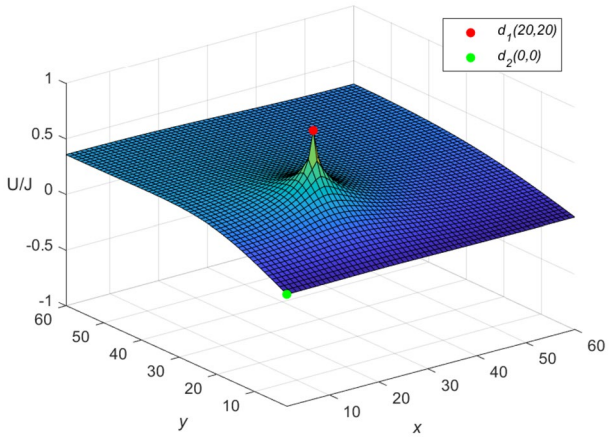

Figure 4. The potential graph for $\mathcal{U}_{60\times 60}(x,y)/J$ with the fan resistor network in Eq. (49).

Idiosyncratic potential formula 2. If the current J flows in from point $d_1(x_1,y_1)$ and out of $d_2(x_2,y_1)$, then a novel potential formula of the cobweb resistor network can be rewritten as

$$\frac{\mathbf{U}_{m\times n}(x,y)}{J}=\frac{4r}{2m+1}\sum_{\iota=1}^{m}\frac{(\mu_{x_1,x}^{(\iota)}-\mu_{x_2,x}^{(\iota)})S_{y_1,\iota}}{U_n^{(\iota)}-U_{n-2}^{(\iota)}-2}S_{y,\iota}, \tag{56}$$

and a novel potential formula of the fan resistor network can be rewritten as

$$\frac{\mathcal{U}_{m\times n}(x,y)}{J}=\frac{4r}{2m+1}\sum_{\iota=1}^{m}\frac{(\varepsilon_{x_1,x}^{(\iota)}-\varepsilon_{x_2,x}^{(\iota)})S_{y_1,\iota}}{(\omega_\iota-2)U_n^{(\iota)}}S_{y,\iota}, \tag{57}$$

where $\mu_{x_s,x}^{(\iota)}$, $\varepsilon_{x_s,x}^{(\iota)}$, $S_{y_s,\iota}$ and $U_v^{(\iota)}$ are same as Eqs. (9), (11), (12) and (14), respectively.

Let $m=n=60$, $J=10$, $y_1=y_2=x_1=20$, $x_2=40$, and $r_0=r=1$ in Eqs. (56) and (57), respectively. Then an idiosyncratic potential formula of the cobweb resistor network is given by

$$\frac{\mathbf{U}_{m\times n}(x,y)}{J}=\frac{4}{121}\sum_{\iota=1}^{60}\frac{(\mu_{20,x}^{(\iota)}-\mu_{40,x}^{(\iota)})S_{20,\iota}}{U_{60}^{(\iota)}-U_{58}^{(\iota)}-2}S_{y,\iota}, \tag{58}$$

$$\mu_{40,x}^{(\iota)}=U_{59-|40-x|}^{(\iota)}+U_{|40-x|-1}^{(\iota)}, \tag{59}$$

and an idiosyncratic potential formula of the fan resistor network is given by

$$\frac{\mathcal{U}_{m\times n}(x,y)}{J}=\frac{4}{121}\sum_{\iota=1}^{60}\frac{(\varepsilon_{20,x}^{(\iota)}-\varepsilon_{40,x}^{(\iota)})S_{20,\iota}}{(\omega_\iota-2)U_{60}^{(\iota)}}S_{y,\iota}, \tag{60}$$

$$\varepsilon_{40,x}^{(\iota)}=(U_{-0.5}^{(\iota)})^2(U_{61-|40-x|}^{(\iota)}-U_{59-|40-x|}^{(\iota)}+U_{20-x}^{(\iota)}-U_{18-x}^{(\iota)}), \tag{61}$$

where $\mu_{20,x}^{(\iota)}$, $\varepsilon_{20,x}^{(\iota)}$, ω_ι, $S_{20,\iota}$ and $S_{y,\iota}$ are expressed in Eqs. (50), (51), (52), (53) and (55), respectively, with $v=61-|20-x|,\ 61-|40-x|,\ 59-|20-x|,\ 59-|40-x|,\ |20-x|-1,\ |40-x|-1,\ 40-x,\ 38-x,\ 20-x,\ 18-x,\ 60,\ 58,\ -0.5,\ \iota=1,2,\ldots,60$

And the three-dimensional dynamic views for the generative process of the potential graph are shown in Figs. 5 and 6 by Matlab.

Idiosyncratic potential formula 3. If the current J/h flows in from point $d_s(x_s,y_1)(s=1,2,\ldots,h)$ and the current J out of $d_2(x_2,y_1)$, then a novel potential formula of the cobweb resistor network can be rewritten as

$$\frac{\mathbf{U}_{m\times n}(x,y)}{J}=\frac{4r}{2m+1}\sum_{\iota=1}^{m}\frac{\sum_{s=1}^{h}\mu_{x_s,x}^{(\iota)}S_{y_1,\iota}-\mu_{x_2,x}^{(\iota)}S_{y_2,\iota}}{U_n^{(\iota)}-U_{n-2}^{(\iota)}-2}S_{y,\iota}, \tag{62}$$

and a novel potential formula of the fan resistor network can be rewritten as

$$\frac{\mathcal{U}_{m\times n}(x,y)}{J}=\frac{4r}{2m+1}\sum_{\iota=1}^{m}\frac{\sum_{s=1}^{h}\varepsilon_{x_s,x}^{(\iota)}S_{y_1,\iota}-\varepsilon_{x_2,x}^{(\iota)}S_{y_2,\iota}}{(\omega_\iota-2)U_n^{(\iota)}}S_{y,\iota}, \tag{63}$$

where $\mu_{x_s,x}^{(\iota)}$, $\varepsilon_{x_s,x}^{(\iota)}$, $S_{y_s,\iota}$ and $U_v^{(\iota)}$ are same as Eqs. (9), (11), (12) and (14), respectively.

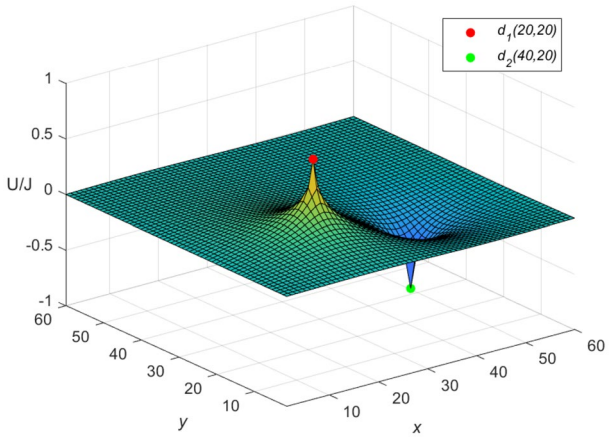

Figure 5. The potential graph for $\mathbf{U}_{60\times 60}(x,y)/J$ with the cobweb resistor network in Eq. (58).

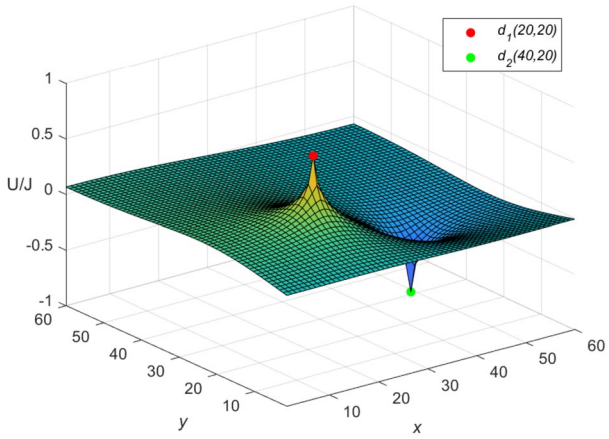

Figure 6. The potential graph for $\mathcal{U}_{60\times 60}(x,y)/J$ with the fan resistor network in Eq. (60).

Let $m=n=60,\ J=10,\ x_1=y_1=20,\ x_2=y_2=40, r_0=r=1$, and $h=10$ in Eqs. (62) and (63), respectively. Then an idiosyncratic potential formula of the cobweb resistor network is represented by

$$\frac{\mathbf{U}_{m\times n}(x,y)}{J}=\frac{4}{121}\sum_{\iota=1}^{60}\frac{\sum_{s=1}^{10}\mu_{x_s,x}^{(\iota)}S_{20,\iota}-\mu_{40,x}^{(\iota)}S_{40,\iota}}{U_{60}^{(\iota)}-U_{58}^{(\iota)}-2}S_{y,\iota}, \tag{64}$$

and an idiosyncratic potential formula of the fan resistor network is represented by

$$\frac{\mathcal{U}_{m\times n}(x,y)}{J}=\frac{4}{121}\sum_{\iota=1}^{60}\frac{\sum_{s=1}^{10}\varepsilon_{x_s,x}^{(\iota)}S_{20,\iota}-\varepsilon_{40,x}^{(\iota)}S_{40,\iota}}{(\omega_\iota-2)U_{60}^{(\iota)}}S_{y,\iota}, \tag{65}$$

$$S_{40,\iota}=\sin\left(\frac{(80\iota-40)\pi}{121}\right), \tag{66}$$

where $\mu_{40,x}^{(\iota)}$, $\varepsilon_{40,x}^{(\iota)}$, ω_ι, $S_{20,\iota}$ and $S_{y,\iota}$ are expressed in Eqs. (59), (61), (52), (53) and (55), respectively, with $v=61-|s-x|$, $61-|40-x|$, $59-|s-x|$, $59-|40-x|$, $|s-x|-1$, $|40-x|-1$, $60-s-x$, $58-s-x$, $20-x$, $18-x$, 60, 58, -0.5, $s=1,2,\ldots,10$. $\iota=1,2,\ldots,60$.

And the three-dimensional dynamic views for the generative process of the potential graph are shown in Figs. 7 and 8 by Matlab.

Idiosyncratic potential formulas with the change of resistivity h ($h=\frac{r}{r_0}$) in resistor network. This section discusses the effect of changes in resistivity h in the resistor network on the potential formulas as reflected in the three-dimensional dynamic view.

Let $m=n=60,\ J=10,\ x_1=y_1=20,\ x_2=y_2=40$, and $r=1$ in Eqs. (8) and (10), respectively. Then an idiosyncratic potential formula of the cobweb resistor network is expressed by

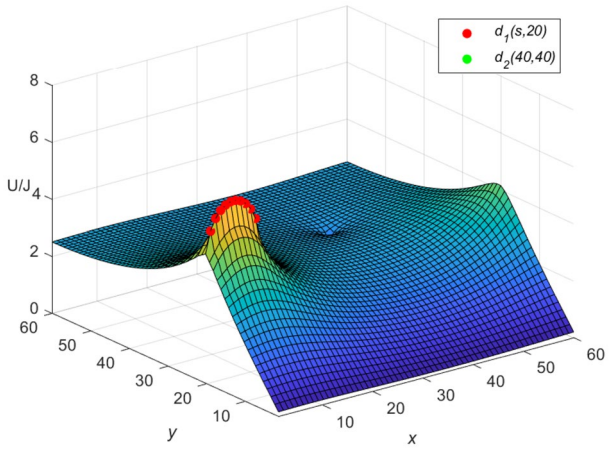

Figure 7. The potential graph for $\mathbf{U}_{60\times60}(x,y)/J$ with the cobweb resistor network in Eq. (64).

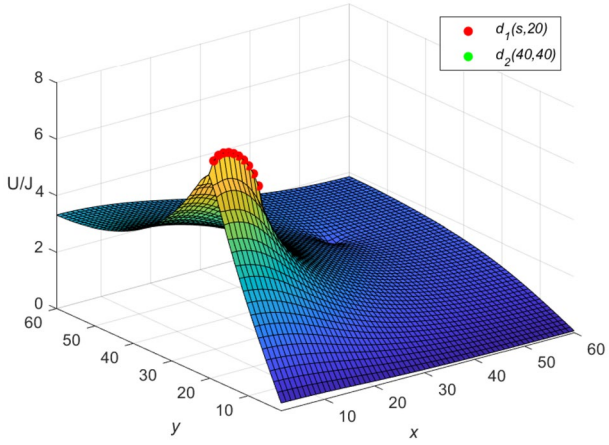

Figure 8. The potential graph for $\mathcal{U}_{60\times60}(x,y)/J$ with the fan resistor network in Eq. (65).

$$\frac{\mathbf{U}_{60\times60}(x,y)}{J}=\frac{4}{121}\sum_{\iota=1}^{60}\frac{\mu_{20,x}^{(\iota)}S_{20,\iota}-\mu_{40,x}^{(\iota)}S_{40,\iota}}{U_{60}^{(\iota)}-U_{58}^{(\iota)}-2}S_{y,\iota}, \tag{67}$$

and an idiosyncratic potential formula of the fan resistor network is expressed by

$$\frac{\mathcal{U}_{60\times60}(x,y)}{J}=\frac{4}{121}\sum_{\iota=1}^{60}\frac{\varepsilon_{20,x}^{(\iota)}S_{20,\iota}-\varepsilon_{40,x}^{(\iota)}S_{40,\iota}}{(\omega_\iota-2)U_{60}^{(\iota)}}S_{y,\iota}, \tag{68}$$

where $\mu_{20,x}^{(\iota)}$, $\mu_{40,x}^{(\iota)}$, $\varepsilon_{20,x}^{(\iota)}$, $\varepsilon_{40,x}^{(\iota)}$, $S_{20,\iota}$, $S_{40,\iota}$ and $S_{y,\iota}$ are expressed in Eqs. (50), (59), (51), (61), (53), (66) and (55), respectively.

Idiosyncratic potential formula 4. When $r_0=10$, $h=0.1$ is got, as h changes, ω_ι and ϕ_ι are obtained as follows, respectively

$$\begin{aligned}\omega_\iota&=2.2-0.2\cos\frac{(2\iota-1)\pi}{121},\\ \cosh\phi_\iota&=1.1-0.1\cos\frac{(2\iota-1)\pi}{121}.\end{aligned} \tag{69}$$

Equation (69) is combined with Eqs. (67) and (68), respectively, and the three-dimensional dynamic views for the generative process of the potential graph are shown in Figs. 9 and 10, respectively.

Idiosyncratic potential formula 5. When $r_0=1, h=1$ is got, as h changes, ω_ι and ϕ_ι are obtained as follows, respectively

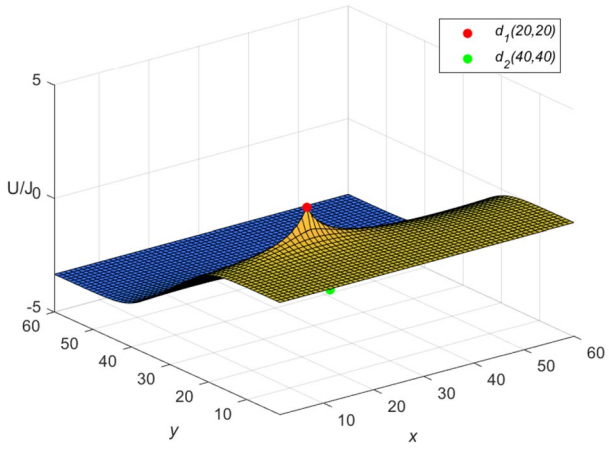

Figure 9. The potential graph for $\mathbf{U}_{60\times 60}(x, y)/J$ with the cobweb resistor network by Eq. (67).

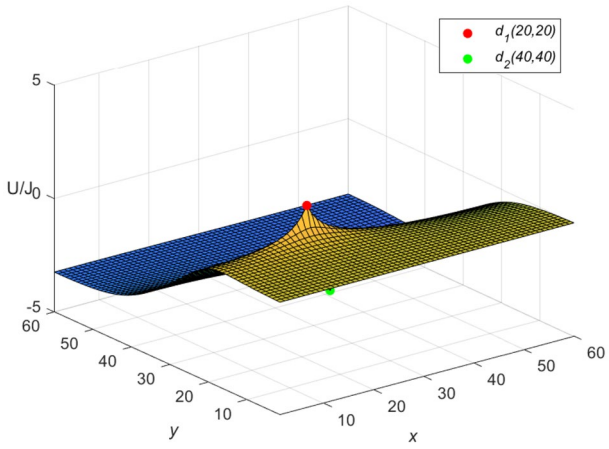

Figure 10. The potential graph for $\mathcal{U}_{60\times 60}(x, y)/J$ with the fan resistor network by Eq. (68).

$$\begin{aligned} \omega_\iota &= 4 - 2\cos\frac{(2\iota-1)\pi}{121}, \\ \cosh\phi_\iota &= 2 - \cos\frac{(2\iota-1)\pi}{121}. \end{aligned} \tag{70}$$

Equation (70) is combined with Eqs. (67) (68), respectively, and the three-dimensional dynamic views for the generative process of the potential graph are shown in Figs. 11 and 12, respectively.

Idiosyncratic potential formula 6. When $r_0 = 0.1$, $h = 10$ is got, as h changes, ω_ι and ϕ_ι are obtained as follows, respectively

$$\begin{aligned} \omega_\iota &= 22 - 20\cos\frac{(2\iota-1)\pi}{121}, \\ \cosh\phi_\iota &= 11 - 10\cos\frac{(2\iota-1)\pi}{121}. \end{aligned} \tag{71}$$

Equation (71) is combined with Eqs. (67) and (68), respectively, and the three-dimensional dynamic views for the generative process of the potential graph are shown in Figs. 13 and 14, respectively.

Numerical algorithms for computing potential

Combining the *DST-VI* and Eqs. (30), (31), (32), (33), (34), this chapter provides two numerical algorithms to achieve fast calculation of large-scale potential for the resistor network. The numerical algorithm obtains similar results to the potential formulas (8) and (10).

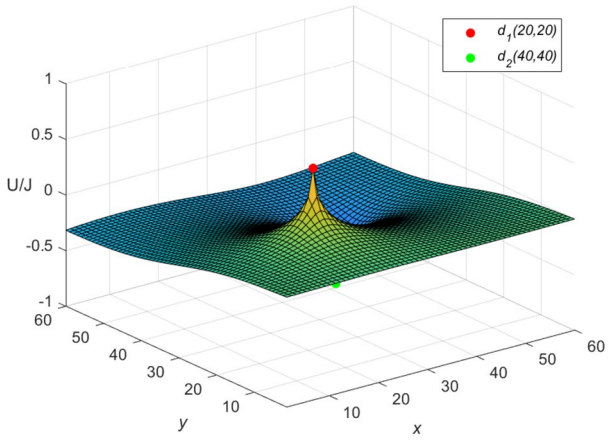

Figure 11. The potential graph for $\mathbf{U}_{60\times 60}(x, y)/J$ with the cobweb resistor network by Eq. (67).

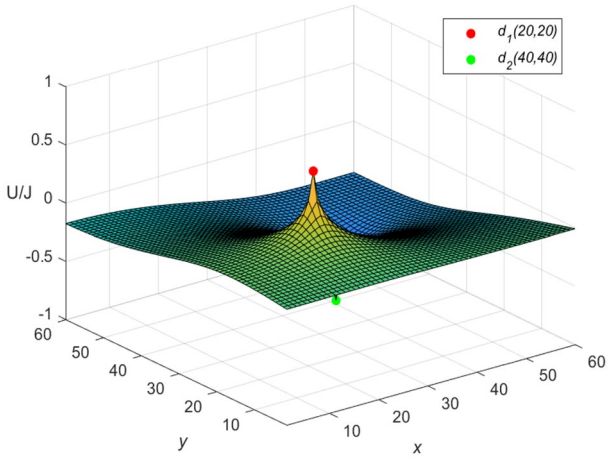

Figure 12. The potential graph for $\mathcal{U}_{60\times 60}(x, y)/J$ with the fan resistor network by Eq. (68).

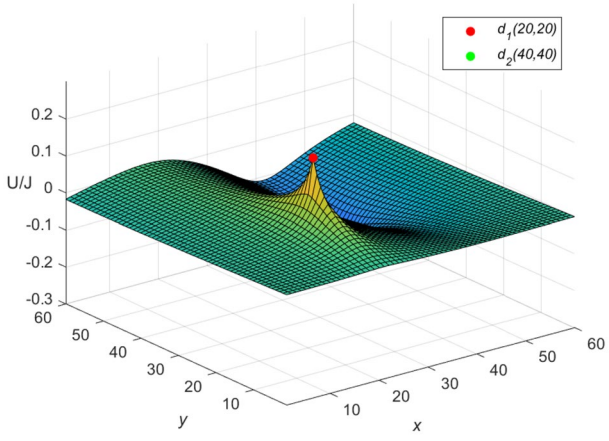

Figure 13. The potential graph for $\mathbf{U}_{60\times 60}(x, y)/J$ with the cobweb resistor network by Eq. (67).

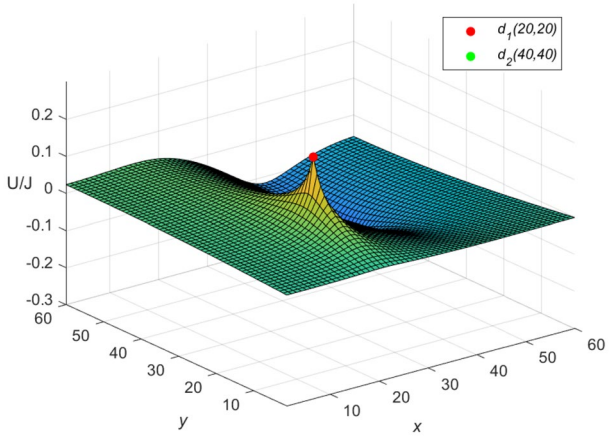

Figure 14. The potential graph for $\mathcal{U}_{60\times 60}(x,y)/J$ with the fan resistor network by Eq. (68).

Algorithm 1: Fast algorithm for matrix and vector multiplication $\mathbf{A}_m\mathbf{q}=\mathbf{y}$

Step 1: Compute y_1 by Eq. $y_1=(2+2h)q_1-hq_2$;
Step 2: Cycle computing y_ι by Eqs. $y_\iota=(-h)q_{\iota-1}+(2+2h)q_\iota-hq_{\iota+1},\ \iota=2,\ldots,m-1$;
Step 3: Compute y_m by Eq. $y_m=(-h)q_{m-1}+(2+h)q_m$.

Algorithm 2: Numerical algorithm for computing $\mathbf{U}_{m\times n}(x,y)/J$ of the cobweb network

Step 1: Compute ω_ι by Eq. (13), $\iota=1,\ 2,\ldots,\ m$;
Step 2: Compute ϕ_ι by $\cosh\phi_\iota=\frac{\omega_\iota}{2},\ \iota=1,\ 2,\ldots,\ m$;
Step 3: Compute $U_v^{(\iota)}$ by Eq. (19), $v=n-|x_s-x|-1,\ |x_s-x|-1,\ n,\ n-2,\ s=1,2.\ \iota=1,\ 2,\ldots,\ m$;
Step 4: Compute $\mathbf{c}_0^{(\iota)}$ and $\mathbf{c}_1^{(\iota)}$ by Eq. (42), $\iota=1,\ldots,\ m$;
Step 5: Compute $\mathbf{V}_v$ by Eq. (38), and *DST-VI*, $v=0,\ 1$;
Step 6: Compute $\mathbf{A}_m\mathbf{V}_v$ by Algorithm 1, $v=1,\ 2,...$;
Step 7: Multiple recursive calculation $\mathbf{V}_v$ by Eq. (35), $v=2,\ 3,\ldots$;
Step 8: Compute $\mathbf{U}_{m\times n}(x,y)/J$ by Eq. (15).

Algorithm 3: Numerical algorithm for computing $\mathcal{U}_{m\times n}(x,y)/J$ of the fan network

Step 1: Compute ω_ι by Eq. (13), $\iota=1,\ 2,\ldots,\ m$;
Step 2: Compute ϕ_ι by $\cosh\phi_\iota=\frac{\omega_\iota}{2},\ \iota=1,\ 2,\ldots,\ m$;
Step 3: Compute $U_v^{(\iota)}$ by Eq. (19),
$v=n-|x_s-x|+1,\ n-|x_s-x|-1,\ n-x_s-x,\ n-x_s-x-2,\ n,\ s=1,\ 2.\ \iota=1,\ 2,\ldots,\ m$;
Step 4: Compute $c_0^{(\iota)}$ and $c_1^{(\iota)}$ by Eq. (45), $\iota=1,\ldots,\ m$;
Step 5: Compute $\mathbf{V}_v$ by Eq. (38) and *DST-VI*, $v=0,\ 1$;
Step 6: Compute $\mathbf{A}_m\mathbf{V}_v$ by Algorithm 1, $v=1,\ 2,...$;
Step 7: Multiple recursive calculation $\mathbf{V}_v$ by Eq. (35), $v=2,\ 3,\ldots$;
Step 8: Compute $\mathcal{U}_{m\times n}(x,y)/J$ by Eq. (15).

Remark 5 As is well-known, the Algorithm 1 is a tridiagonal matrix-vector multiplication, which the computational complexity is $O(n)$. Moreover, one *DST-VI* needs $2n\log_2 n+O(n)$ real arithmetic operations[68]. So the Algorithm 2 composed of Algorithm 1 and two *DST-VI*, and it's computational complexity is $4n\log_2 n+O(n)$. Analogous, the computational complexity of Algorithms 3 is also $4n\log_2 n+O(n)$. According to the above Algorithms 2 and Algorithms 3, two instances are used to display the iterative effect of large-scale data graphically in the following.

Let $m=400$ and $n=10$, the current J flows from the $d_1(x_1,y_1)$ point, $x_1=3,y_1=150$, and out from the $d_2(x_2,y_2)$ point, $x_2=7,y_2=350$. $r=1,r_0=100$, and $J=10$. The fast algorithm of cobweb resistor network is shown in Fig. 15, and the fast algorithm of fan resistor network is shown in Fig. 16.

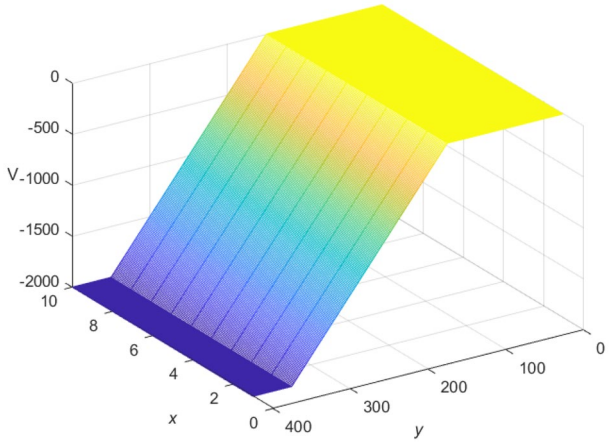

Figure 15. A 3D image display for the fast Algorithm 2 of $\mathbf{U}_{400\times10}(x, y)/J$ on the cobweb resistor network.

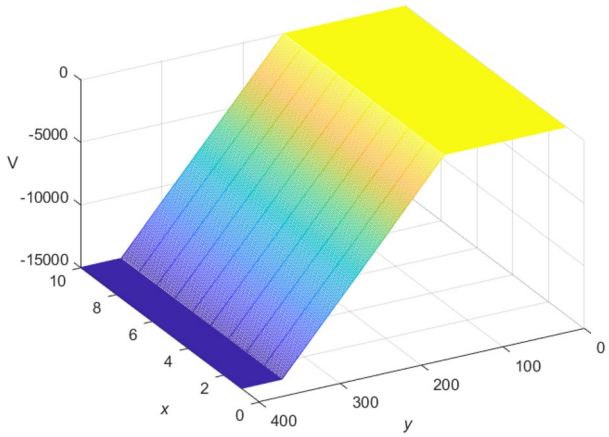

Figure 16. A 3D image display for the fast Algorithm 3 of $\mathcal{U}_{400\times10}(x, y)/J$ on the fan resistor network.

Efficiency of calculation method

On the $m \times n$ scale resistor network models, (x_1, y_1) refers to the input point of the current and (x_2, y_2) refers to the output point of the current. We give a comparison of calculation efficiency for the calculating potential in three different methods. "Time" is the total CPU time in seconds, t_1, t_2 and t_3 denote CPU times of the potential computed by formulas (1), (3), formulas (8), (10) and Algorithm 2, 3, respectively.

The experiment is completed under the environmental conditions of CPU model AMD R9-5900HX, CPU frequency 3.30 GHz, and Matlab version is R2020b. "$m \times n$" is the number of nodes in the resistor network., " — " denotes the operation time more than 1200s or beyond the memory limit of Matlab.

$m \times n$	(x_1, y_1)	(x_2, y_2)	r/r_0	t_1	t_2
100 × 100	(40 , 40)	(80 , 80)	1	0.139	0.029
200 × 200	(40 , 40)	(180 , 180)	1	0.923	0.121
300 × 300	(40 , 40)	(180 , 180)	1	2.817	0.340
400 × 400	(40 , 40)	(180 , 180)	1	7.685	1.649
800 × 100	(40 , 40)	(80 , 80)	1	6.652	0.874
800 × 200	(40 , 40)	(180 , 180)	1	15.269	3.510

Table 1. The comparison of calculation efficiency for potential formulas (1) and (8).

$m \times n$	(x_1, y_1)	(x_2, y_2)	r/r_0	t_1	t_2
100 × 100	(40 , 40)	(80 , 80)	1	0.271	0.045
200 × 200	(40 , 40)	(180 , 180)	1	1.667	0.244
300 × 300	(40 , 40)	(180 , 180)	1	–	0.631
400 × 400	(40 , 40)	(180 , 180)	1	–	2.964
800 × 100	(40 , 40)	(80 , 80)	1	13.210	1.546
800 × 200	(40 , 40)	(180 , 180)	1	30.351	5.925

Table 2. The comparison of calculation efficiency for potential formulas (3) and (10).

$m \times n$	(x_1, y_1)	(x_2, y_2)	r/r_0	t_1	t_2
400 × 400	(40 , 40)	(180 , 180)	0.1	7.626	1.760
500 × 500	(40 , 40)	(180 , 180)	0.1	14.666	3.001
600 × 600	(40 , 40)	(180 , 180)	0.1	25.365	4.932
1100 × 1100	(40 , 40)	(180 , 180)	0.1	159.767	34.444
1000 × 400	(40 , 40)	(180 , 180)	0.1	47.323	9.187
1000 × 500	(40 , 40)	(180 , 180)	0.1	59.539	11.613

Table 3. The comparison of calculation efficiency for potential formulas (1) and (8).

$m \times n$	(x_1, y_1)	(x_2, y_2)	r/r_0	t_1	t_2
400 × 400	(40 , 40)	(180 , 180)	0.1	14.962	3.016
500 × 500	(40 , 40)	(180 , 180)	0.1	28.453	5.325
600 × 600	(40 , 40)	(180 , 180)	0.1	–	9.052
1100 × 1100	(40 , 40)	(180 , 180)	0.1	–	63.093
1000 × 400	(40 , 40)	(180 , 180)	0.1	91.827	16.498
1000 × 500	(40 , 40)	(180 , 180)	0.1	118.262	20.461

Table 4. The comparison of calculation efficiency for potential formulas (3) and (10).

$m \times n$	(x_1, y_1)	(x_2, y_2)	r/r_0	t_1	t_2
1000 × 1000	(40 , 40)	(580 , 580)	0.01	120.787	25.788
1500 × 1500	(40 , 40)	(580 , 580)	0.01	405.983	92.694
1800 × 1800	(40 , 40)	(580 , 580)	0.01	700.525	159.449
2000 × 2000	(40 , 40)	(580 , 580)	0.01	958.713	217.022
1500 × 1000	(40 , 40)	(580 , 580)	0.01	270.714	61.578
2000 × 1000	(40 , 40)	(580 , 580)	0.01	480.070	110.790

Table 5. The comparison of calculation efficiency for potential formulas (1) and (8).

Remark 6 Tables 1, 3, 5 show the calculation time of cobweb resistor network with different square and rectangular sizes at different resistivity. The optimized potential formula (8) has faster operation speed.

Remark 7 Tables 2, 4, 6 show the calculation time of fan resistor network with different square and rectangular sizes at different resistivity. The optimized potential formula (10) has faster operation speed.

Remark 8 Table 7 shows the efficiency of the potential formula (1), formula (8) and the Algorithm 2 for calculating the potential. Algorithm 2 not only realizes large-scale calculation, but also has shorter calculation time in calculating cobweb resistor network.

Remark 9 Table 8 shows the efficiency of the potential formula (3), formula (10) and the Algorithm 3 for calculating the potential. Algorithm 3 not only realizes large-scale calculation, but also has shorter calculation time in calculating fan resistor network.

$m \times n$	(x_1, y_1)	(x_2, y_2)	r/r_0	t_1	t_2
1000 × 1000	(40 , 40)	(580 , 580)	0.01	234.791	46.840
1500 × 1500	(40 , 40)	(580 , 580)	0.01	792.929	171.828
1800 × 1800	(40 , 40)	(580 , 580)	0.01	1373.612	308.328
2000 × 2000	(40 , 40)	(580 , 580)	0.01	–	410.130
1500 × 1000	(40 , 40)	(580 , 580)	0.01	528.783	114.033
2000 × 1000	(40 , 40)	(580 , 580)	0.01	943.748	208.219

Table 6. The comparison of calculation efficiency for potential formulas (3) and (10).

$m \times n$	(x_1, y_1)	(x_2, y_2)	r/r_0	t_1	t_2	t_3
100 × 10	(3 , 30)	(5 , 50)	0.01	0.031	0.013	0.013
1000 × 10	(3 , 300)	(5 , 500)	0.01	1.144	0.213	0.033
10000 × 10	(3 , 3000)	(5 , 5000)	0.01	105.350	11.588	1.098
20000 × 10	(3 , 3000)	(5 , 5000)	0.01	474.890	93.546	4.156
30000 × 10	(3 , 3000)	(5 , 5000)	0.01	1043.302	204.098	8.369
40000 × 10	(3 , 3000)	(5 , 5000)	0.01	1857.076	358.305	19.710

Table 7. Comparison of the efficiency for potential formulas (1), (8) and Algorithm 2.

$m \times n$	(x_1, y_1)	(x_2, y_2)	r/r_0	t_1	t_2	t_3
100 × 10	(3 , 30)	(5 , 50)	0.01	0.035	0.017	0.013
1000 × 10	(3 , 300)	(5 , 500)	0.01	1.188	0.388	0.050
10000 × 10	(3 , 3000)	(5 , 5000)	0.01	106.246	21.425	1.014
20000 × 10	(3 , 3000)	(5 , 5000)	0.01	468.767	175.736	3.465
30000 × 10	(3 , 3000)	(5 , 5000)	0.01	1041.555	365.012	7.998
40000 × 10	(3 , 3000)	(5 , 5000)	0.01	1858.145	637.289	19.353

Table 8. Comparison of the efficiency for potential formulas (3), (10) and Algorithm 3.

Conclusion

In this paper, based on the *RT-V* method, the accurate potential formulas of the $m \times n$ cobweb resistor network and the $m \times n$ fan resistor network[1] are improved. The potential formula is represented by the Chebyshev polynomial of the second class and the tridiagonal matrix is diagonalized by the *DST-VI* method, which realizes the high efficiency of the numerical simulation of the potential formula. The changes of variables in the potential formula are analyzed, and the corresponding three-dimensional view is drawn to show the influence of variable changes on the image. Then we design a fast algorithm for the resistor network potential to achieve fast calculation in the case of large-scale resistor networks. Finally, we show the calculation time of different calculation methods under different scale resistor networks, and the comparison shows the efficiency of the improved numerical simulation calculation.

Data availability

All data generated or analysed during this study are included in this article and its supplementary information files.

Received: 25 April 2023; Accepted: 26 July 2023
Published online: 31 July 2023

References

1. Tan, Z.-Z. Recursion-transform method and potential formulae of the $m \times n$ cobweb and fan networks. *Chin. Phys. B.* **26**(9), 090503 (2017).
2. Hadad, Y., Soric, J. C., Khanikaev, A. B. & Alù, A. Self-induced topological protection in nonlinear circuit arrays. *Nat. Electron.* **1**, 178–182 (2018).
3. Zhang, D. *et al.* Impact damage localization and mode identification of CFRPs panels using an electric resistance change method. *Compos. Struct.* **276**, 114587 (2021).
4. Kirchhoff, G. Ueber die Aufölsung der Gleichungen, auf welche man bei der Untersuchung der linearen Vertheilung galvanischer Ströme geführt wird. *Ann. Phys.* **148**, 497–508 (1847).
5. Winstead, V. & Demarco, C. L. Network essentiality. *IEEE Trans. Circuits-I.* **60**(3), 703–709 (2012).

6. Ferri, G. & Antonini, G. Ladder-network-based model for interconnects and transmission lines time delay and cutoff frequency determination. *J. Circuit. Syst. Comput.* **16**, 489–505 (2007).
7. Owaidat, M. Q., Hijjawi, R. S. & Khalifeh, J. M. Network with two extra interstitial resistors. *Int. J. Theor. Phys.* **51**, 3152–3159 (2012).
8. Kirkpatrick, S. Percolation and Conduction. *Rev. Mod. Phys.* **45**, 497–508 (1973).
9. Katsura, S. & Inawashiro, S. Lattice Green's functions for the rectangular and the square lattices at arbitrary points. *J. Math. Phys.* **12**, 1622 (1971).
10. Pennetta, C. *et al.* Biased resistor network model for electromigration failure and related phenomena in metallic lines. *Phys. Rev. B.* **70**, 174305 (2004).
11. Kook, W. Combinatorial Green's function of a graph and applications to networks. *Adv. Appl. Math.* **46**, 417–423 (2011).
12. Shi, Y. *et al.* Novel discrete-time recurrent neural networks handling discrete-form time-variant multi-augmented Sylvester matrix problems and manipulator application. *IEEE Trans. Neur. Net. Lear.* **33**(2), 587–599 (2022).
13. Shi, Y., Zhao, W.-H., Li, S., Li, B. & Sun, X.-B. Novel discrete-time recurrent neural network for robot manipulator: a direct discretization technical route. *IEEE Trans. Neur. Net. Lear.* (2021). https://doi.org/10.1109/TNNLS.2021.3108050
14. Liu, K.-P. *et al.* Five-step discrete-time noise-tolerant zeroing neural network model for time-varying matrix inversion with application to manipulator motion generation. *Eng. Appl. Artif. Intel.* **103**, 104306 (2021).
15. Sun, Z.-B. *et al.* Noise-suppressing zeroing neural network for online solving time-varying matrix square roots problems: A control-theoretic approach. *Expert. Syst. Appl.* **192**, 116272 (2022).
16. Jin, L., Qi, Y.-M., Luo, X., Li, S. & Shang, M.-S. Distributed competition of multi-robot coordination under variable and switching topologies. *IEEE Trans. Autom. Sci. Eng.* **19**(4), 3575–3586 (2022).
17. Jin, L., Zhang, Y.-N., Li, S. & Zhang, Y.-Y. Modified ZNN for time-varying quadratic programming with inherent tolerance to noises and its application to kinematic redundancy resolution of robot manipulators. *IEEE T. Ind. Electron.* **63**(11), 6978–6988 (2016).
18. Jin, L., Zheng, X. & Luo, X. Neural dynamics for distributed collaborative control of manipulators with time delays. *IEEE-CAA J. Autom.* **9**(5), 854–863 (2022).
19. Klein, D. J., & Randić, M. Resistance distance. *J. Math. Chem.* **12**, 81–95 (1993).
20. Cserti, J. Application of the lattice Green's function for calculating the resistance of an infinite network of resistors. *Am. J. Phys.* **68**, 896–906 (2000).
21. Giordano, S. Disordered lattice networks: general theory and simulations. *Int. J. Circ. Theor. App.* **33**, 519–540 (2005).
22. Wu, F. Y. Theory of resistor networks: The two-point resistance. *J. Phys. A: Math. Gen.* **37**, 6653 (2004).
23. Tzeng, W. J. & Wu, F. Y. Theory of impedance networks: The two-point impedance and LC resonances. *J. Phys. A: Math. Gen.* **39**, 8579 (2006).
24. Essam, J. W. & Wu, F. Y. The exact evaluation of the corner-to-corner resistance of an $M \times N$ resistor network: Asymptotic expansion. *J. Phys. A : Math. Theor.* **42**, 025205 (2008).
25. Izmailian, N. S. & Huang, M.-C. Asymptotic expansion for the resistance between two maximum separated nodes on an M by N resistor network. *Phys. Rev. E.* **82**, 011125 (2010).
26. Lai, M.-C. & Wang, W.-C. Fast direct solvers for Poisson equation on 2D polar and spherical geometries. *Numer. Meth. Part. D. E.* **18**, 56–68 (2002).
27. Borges, L. & Daripa, P. A fast parallel algorithm for the Poisson equation on a disk. *J. Comput. Phys.* **169**, 151–192 (2001).
28. Izmailian, N. S., Kenna, R. & Wu, F. Y. The two-point resistance of a resistor network: A new formulation and application to the cobweb network. *J. Phys. A: Math. Theor.* **47**, 035003 (2014).
29. Izmailian, N. S. & Kenna, R. A generalised formulation of the Laplacian approach to resistor networks. *J. Stat. Mech : Theor. E.* **9**, 1742–5468 (2014).
30. Izmailian, N. S. & Kenna, R. The two-point resistance of fan networks. *Chin. J. Phys.* **53**(2), 040703 (2015).
31. Chair, N. Trigonometrical sums connected with the chiral Potts model, Verlinde dimension formula, two-dimensional resistor network, and number theory. *Ann. Phys.* **341**, 56–76 (2014).
32. Chair, N. The effective resistance of the N-cycle graph with four nearest neighbors. *J. Stat. Phys.* **154**, 1177–1190 (2014).
33. Tan, Z.-Z., Zhou, L. & Yang, J.-H. The equivalent resistance of a $3 \times n$ cobweb network and its conjecture of an $m \times n$ cobweb network. *J. Phys. A: Math. Theor.* **46**(19), 195202 (2013).
34. Tan, Z.-Z. Recursion-transform approach to compute the resistance of a resistor network with an arbitrary boundary. *Chin. Phys. B.* **24**(2), 020503 (2015).
35. Tan, Z.-Z. Recursion-transform method for computing resistance of the complex resistor network with three arbitrary boundaries. *Phys. Rev. E.* **91**(5), 052122 (2015).
36. Tan, Z.-Z. Recursion-transform method to a non-regular $m \times n$ cobweb with an arbitrary longitude. *Sci. Rep.* **5**, 11266 (2015).
37. Tan, Z.-Z., Essam, J. W. & Wu, F. Y. Two-point resistance of a resistor network embedded on a globe. *Phys. Rev. E.* **90**(1), 012130 (2014).
38. Essam, J. W., Tan, Z.-Z. & Wu, F. Y. Resistance between two nodes in general position on an $m \times n$ fan network. *Phys. Rev. E.* **90**(3), 032130 (2014).
39. Tan, Z.-Z. & Fang, J.-H. Two-point resistance of a cobweb network with a $2r$ boundary. *Commun. Theor. Phys.* **63**(1), 36–44 (2015).
40. Tan, Z.-Z. Theory on resistance of $m \times n$ cobweb network and its application. *Int. J. Circ. Theor. Appl.* **43**(11), 1687–1702 (2015).
41. Tan, Z.-Z. Two-point resistance of a non-regular cylindrical network with a zero resistor axis and two arbitrary boundaries. *Commun. Theor. Phys.* **67**(3), 280–288 (2017).
42. Tan, Z.-Z. Two-point resistance of an $m \times n$ resistor network with an arbitrary boundary and its application in RLC network. *Chin. Phys. B.* **25**(5), 050504 (2016).
43. Tan, Z., Tan, Z.-Z. & Chen, J. Potential formula of the nonregular $m \times n$ fan network and its application. *Sci. Rep.* **8**, 5798 (2018).
44. Tan, Z. & Tan, Z.-Z. Potential formula of an $m \times n$ globe network and its application. *Sci. Rep.* **8**(1), 9937 (2018).
45. Tan, Z.-Z. & Tan, Z. Electrical properties of an arbitrary $m \times n$ rectangular network. *Acta Phys. Sin.* **62**(2), 020502 (2020).
46. Tan, Z.-Z. Resistance theory for two classes of n-periodic networks. *Eur. Phys. J. Plus* **137**(5), 1–12 (2022).
47. Tan, Z.-Z. & Tan, Z. Electrical properties of $m \times n$ cylindrical network. *Chin. Phys. B.* **29**(8), 080503 (2020).
48. Tan, Z.-Z. & Tan, Z. The basic principle of $m \times n$ resistor networks. *Commun. Theor. Phys.* **72**(5), 055001 (2020).
49. Fang, X.-Y. & Tan, Z.-Z. Circuit network theory of n-horizontal bridge structure. *Sci. Rep.* **12**(1), 6158 (2022).
50. Tan, Z.-Z. Electrical property of an $m \times n$ apple surface network. *Results Phys.* **47**, 106361 (2023).
51. Luo, X.-L. & Tan, Z.-Z. Fractional circuit network theory with n-V-structure. *Phys. Scr.* **98**(4), 045224 (2023).
52. Tan, Z.-Z. Theory of an $m \times n$ apple surface network with special boundary. *Commun. Theor. Phys.* **75**(6), 065701 (2023).
53. Zhou, S., Wang, Z.-X., Zhao, Y.-Q. & Tan, Z.-Z. Electrical properties of a generalized $2 \times n$ resistor network. *Commun. Theor. Phys.* **75**, 075701 (2023).
54. Fu, Y.-R., Jiang, X.-Y., Jiang, Z.-L. & Jhang, S. Properties of a class of perturbed Toeplitz periodic tridiagonal matrices. *Comp. Appl. Math.* **39**, 1–19 (2020).
55. Fu, Y.-R., Jiang, X.-Y., Jiang, Z.-L. & Jhang, S. Inverses and eigenpairs of tridiagonal Toeplitz matrix with opposite-bordered rows. *J. Appl. Anal. Comput.* **10**(4), 1599–1613 (2020).

56. Fu, Y.-R., Jiang, X.-Y., Jiang, Z.-L. & Jhang, S. Analytic determinants and inverses of Toeplitz and Hankel tridiagonal matrices with perturbed columns. *Spec. Matrices.* **8**, 131–143 (2020).
57. Wei, Y.-L., Zheng, Y.-P., Jiang, Z.-L. & Shon, S. The inverses and eigenpairs of tridiagonal Toeplitz matrices with perturbed rows. *J. Appl. Math. Comput.* **68**, 623–636 (2022).
58. Wei, Y.-L., Jiang, X.-Y., Jiang, Z.-L. & Shon, S. On inverses and eigenpairs of periodic tridiagonal Toeplitz matrices with perturbed corners. *J. Appl. Anal. Comput.* **10**(1), 178–191 (2020).
59. Wei, Y.-L., Zheng, Y.-P., Jiang, Z.-L. & Shon, S. A study of determinants and inverses for periodic tridiagonal Toeplitz matrices with perturbed corners involving Mersenne numbers. *Mathematics.* **7**(10), 893 (2019).
60. Wei, Y.-L., Jiang, X.-Y., Jiang, Z.-L. & Shon, S. Determinants and inverses of perturbed periodic tridiagonal Toeplitz matrices. *Adv. Differ. Equ.* **2019**(1), 410 (2019).
61. Zhou, Y.-F., Zheng, Y.-P., Jiang, X.-Y. & Jiang, Z.-L. Fast algorithm and new potential formula represented by Chebyshev polynomials for an $m \times n$ globe network. *Sci. Rep.* **12**(1), 21260 (2022).
62. Mason, J. C. & Handscomb, D. C. *Chebyshev Polynomials*. (Chapman & Hall/CRC, 2002).
63. Udrea, G. A note on the sequence $(W_n)_{n\geq 0}$ of A.F. Horadam. *Port. Math.* **53**, 143–156 (1996).
64. Garcia, S. R. & Yih, S. Supercharacters and the discrete Fourier, cosine, and sine transforms. *Commun. Algebra.* **46**(9), 3745–3765 (2018).
65. Sanchez, V., Garcia, P., Peinado, A. M., Segura, J. C. & Rubio, A. J. Diagonalizing properties of the discrete cosine transforms. *IEEE Trans. Signal. Process.* **43**(11), 2631–2641 (1995).
66. Strang, G. The discrete cosine transform. *SIAM. Rev.* **41**(1), 135–147 (1999).
67. Liu, Z., Chen, S., Xu, W. & Zhang, Y. The eigen-structures of real (skew) circulant matrices with some applications. *Comput. Appl. Math.* **38**, 178 (2019).
68. Yip, P. C. & Rao, K. R. DIF algorithms for DCT and DST. *IEEE Int. Conf. Acoust. Speech and Signal Processing.* 776–779. http://dx.doi.org/10.1109/ICASSP.1985.1168246 (1985).

Acknowledgements

The research was supported by the National Natural Science Foundation of China (Grant No.12001257), the Natural Science Foundation of Shandong Province (Grant No. ZR2020QA035).

Author contributions

Zheng, Yan-Peng and Jiang, Xiao-Yu conceived the project, performed and analyzed formulae calculations. Zhao, Wen-Jie validated the correctness of the formula calculation, and realized the numerical simulation and graph drawing. Jiang, Zhao-Lin present the fast algorithm of computing potential. All authors contributed equally to the manuscript.

Competing interests

The authors declare no competing interests.

Additional information

Correspondence and requests for materials should be addressed to Y.Z. or Z.J.

Reprints and permissions information is available at www.nature.com/reprints.

Publisher's note Springer Nature remains neutral with regard to jurisdictional claims in published maps and institutional affiliations.